Poly(arylene ether) electrolyte membranes bearing aliphatic-chain-linked sulfophenyl pendant groups

Zhang, Qiang; Liu, Baijun; Hu, Wei; Xu, Wan; Jiang, Zhenhua; Xing, Wei; Guiver, Michael D.

Publisher's version / Version de l'éditeur:
https://doi.org/10.1016/j.memsci.2012.08.044
Journal of Membrane Science, 428, pp. 629-638, 2012-09-03

Poly(arylene ether) electrolyte membranes bearing aliphatic-chain-linked sulfophenyl pendant groups

Qiang Zhang [a], Baijun Liu [a], Wei Hu [a], Wan Xu [a], Zhenhua Jiang [a,*], Wei Xing [b], and Michael D. Guiver [c,d]

[a] *College of Chemistry, Jilin University, 2699 Qianjin Street, Changchun 130012, P.R. China*
[b] *Changchun Institute of Applied Chemistry, Chinese Academy of Sciences, 5625 Renmin Street, Changchun 130022, P.R. China*
[c] *National Research Council, 1200 Montreal Road, Ottawa, Ontario K1A 0R6, Canada*
[d] *Department of Energy Engineering, Hanyang University, 17 Haengdang-dong, Seongdong-gu, Seoul 133-791, S. Korea*

*Corresponding author: Zhenhua Jiang
e-mail: jiangzhenhua@jlu.edu.cn
Tel: +86 431 85168886
Fax: +86 431 85168868

Abstract:

Two series of novel side-chain-acid poly(arylene ether)s bearing aliphatic-chain-linked sulfophenyl pendants are synthesized by direct polycondensation reactions derived from a new sulfonated difluoro-monomer, 4-(3-(4-(2,6-difluorobenzoyl)-phenoxy)benzenesulfonate. The sulfonation content is readily controlled by adjusting the feed ratios of sulfonated and unsulfonated monomers. The obtained polymers exhibit considerably reduced dimensional swelling and good proton conductivities. It is found that the cyano-functionalized poly(arylene ether)s exhibit lower water uptake and dimensional swelling in comparison with the corresponding SPAE series. SPAEK-3 with an ion exchange capacity of 1.5 mequiv g^{-1} has proton conductivity of 0.12 S cm^{-1} and water swelling ratio of only 26 % at 100 ^{o}C. Importantly, obvious hydrophobic/hydrophilic phase separation morphology is observed, which may be highly related with their good proton transport ability.

Keywords: poly(arylene ether)s, proton exchange membranes, morphology, fuel cells.

1. Introduction

Fuel cells are regarded as one of the promising clean future power sources for their low emissions and high conversion efficiency [1-3]. Proton exchange membranes (PEMs) are attracting increasing attention due to being key components of environmentally-benign fuel cells [4-7]. Among all kinds of proton conducting polymer electrolytes that have been reported, perfluorinated sulfonic acid ionomers such as Nafion ® (DuPont™) and Dow membrane (DOW) brought about a major breakthrough in proton exchange membrane fuel cells (PEMFCs) and direct methanol fuel cells (DMFCs). However, high cost, high methanol crossover, constrained operation temperature (≤ 80 °C), and environmental recycling uncertainties of Nafion and other similar perfluorinated membranes are limiting their widespread commercial application in fuel cells [8-9]. Consequently, many efforts have been made to design and synthesize alternative PEM materials to replace the perfluorosulfonic acid ones.

Sulfonated aromatic polymers, derived from polymers such as poly(arylene ether ketone)s, poly(arylene ether sulfone)s, polyimides, poly(arylene ether nitrile)s and poly(benzimidazole)s, are among the most promising candidates as alternative PEM materials due to their high thermal and chemical stability, high proton conductivity and low methanol permeability [10-21]. However, in comparison with perfluorosulfonic acid membranes, sulfonated aromatic PEMs often have lower proton conductivity, which is largely related to their weaker acidity and poor hydrophilic and hydrophobic phase separation [22]. Although numerous non-perfluorinated sulfonated polyaromatics have been prepared for PEMs, only a few of them exhibited comparable performance to Nafion [22-27].

Aimed at preparing PEMs having ideal microstructure for enhanced proton conduction, some approaches have been tried. Generally, the block copolymers showed better trend to form hydrophobic/hydrophilic phase separation than those of random polymers. McGrath reported a series of PAES–PBP multiblock copolymers, which showed clear phase separation and improved proton conductivity [28]. Holdcroft prepared some SPSF-block-PVDF and PS-block-PSSNa polymers having ideal microstructure and good proton conductivity [29]. Li et al. recently reported aromatic A-B-A triblock polymers, which exhibited connected proton-conducting channels [30]. It appears that the unique polymer chemical structure is also helpful to induce nanophase separation, which is responsible for the high proton conductivity. Comb-shaped polymers having rigid aromatic main chains and flexible side chains were prepared by Norsten et al., and these PEMs displayed excellent proton transport ability [31]. However, this required a multi-step synthetic procedure. Recently, Li et al. reported aromatic comb-shaped polymers based on sulfonated poly(phenylene oxide) side chains, which exhibited well-defined nanophase separation [32]. The membranes exhibited excellent proton transport ability.

In this study, two series of polyarylether-type polymers having sulfophenyl pendant connected by a flexible –O–$(CH_2)_3$–O– linkage were synthesized through a direct polymerization of a new sulfonated difluoro-monomer. Different from our previously reported mainchain-acid and side-group-acid PEMs (Scheme 1), the present polymers contained flexible side chains terminated by sulfophenyl pendants.

This structural design was intended to induce and improve the formation of hydrophobic/hydrophilic phase separation. The properties relevant to PEM applications were fully investigated.

2. Experimental

2.1. Chemicals and Materials

2,6-Difluorobenzoyl chloride and 1,3-diphenoxyalkanes were synthesized in our laboratory using standard methods [33]. 1,3-Dibromoalkane and 2,6-difluorobenzonitrile were purchased from Aladdin-reagent. 4,4'-Difluorobenzophenone (DFBP), phenol and NaOH were purchased from Beijing Chemical Factory. K_2CO_3 (Beijing Chemical Factory) was ground into fine powder and dried at 120 ^oC for 24 h before use. All the other organic solvents were obtained from commercial sources and purified by conventional methods.

2.2. Synthesis of the Monomers

2.2.1. Synthesis of (2,6-Difluorophenyl)(4-(3-phenoxypropoxy)phenyl)methanone (DPPM):

A 250 mL three-neck flask equipped with a mechanical stirrer, a dropping funnel, and a nitrogen inlet was charged with 1-(3-phenoxypropoxy)benzene (25 g, 0.11 mol) and CH_2Cl_2 (75 mL). The solution was cooled to 0 °C, and anhydrous $AlCl_3$ (14.6 g, 0.11 mol) was added in several portions. After the solution was stirred for 10 min, 2,6-difluorobenzoyl chloride (17.6 g, 0.1 mol) was added dropwise over 10 min. The solution was stirred at 0 °C for 4 h and poured into 100 mL of 1 M hydrochloric acid ice-water solution. The organic phase was separated and washed with 10% NaOH (100 mL) and H_2O (400 mL). The solution was dried with anhydrous $MgSO_4$, and the solvent was evaporated in vacuum. After being recrystallized in petroleum (60-90 °C) and dried, 16 g of white crystals was obtained. Yield: 89%.

FT-IR (KBr): 1669 cm^{-1} (C=O).

^{1}H NMR (300 MHz, DMSO-d_6) δ (ppm): 7.78 (d, *J* = 8.8 Hz, 2H), 7.67 (tt, *J* = 8.2, 6.7 Hz, 1H), 7.36 – 7.22 (m, 4H), 7.15 (dd, *J* = 6.9, 4.9 Hz, 2H), 7.01 – 6.88 (m, 3H), 4.27 (t, *J* = 6.2 Hz, 2H), 4.13 (t, *J* = 6.2 Hz, 2H), 2.21 (p, *J* = 6.2 Hz, 2H).

2.2.2. Synthesis of Sodium 4-(3-(4-(2,6-Difluorobenzoyl)phenoxy)propoxy)benzenesulfonate (SDPPM):

DPPM (5 g, 13.6 mmol) was dissolved in 34 mL of anhydrous CH_3Cl. The solution was cooled to 0 °C, and chlorosulfonic acid (4.75 g, 54.4 mmol) was added in several portions. The red solution was stirred at room temperature for 24 h, and then excess 10% NaOH aqueous solution was added into the solution. The resulting precipitate was filtered, recrystallized in water and dried in a vacuum oven at 120 °C for 24 h. Yield: 90%.

FT-IR (KBr): 1034 cm^{-1}, 1127 cm^{-1} (–SO_3Na), 1 660 cm^{-1} (C=O), 1257 cm^{-1}(C–O–C).

^{1}H NMR (300 MHz, DMSO-d_6) δ (ppm): 7.78 (d, *J* = 8.4 Hz, 2H), 7.65 (d, *J* = 7.1 Hz, 1H), 7.52 (d, *J* = 8.3 Hz, 2H), 7.30 (t, *J* = 8.1 Hz, 2H), 7.14 (d, *J* = 8.7 Hz, 2H), 6.88

(d, *J* = 8.5 Hz, 2H), 4.26 (t, *J* = 5.9 Hz, 2H), 4.14 (t, *J* = 5.7 Hz, 2H), 2.41 – 1.98 (m, 2H).

2.3. Synthesis of Polymers

The side-chain-type sulfonated poly(arylene ether) copolymers, SPAE and SPAEN, were synthesized by polycondensation reaction. A typical synthesis procedure of SPAE-3 was as follows. A 100 mL three-neck round-bottomed flask equipped with a nitrogen inlet and a dropping funnel was charged with SDPPM (4.33 g, 0.092 mol), DFBP (1.75 g, 0.008 mol), DHDPE (4.04 g, 0.02 mol), potassium carbonate (3.080 g, 0.022mol), toluene (10 mL) and tetramethylene sulfone (TMS, 40 mL). The mixture was kept at room temperature for a few minutes and then heated to 140 °C within 3 h. After stirring at 180 °C for 6 h in nitrogen atmosphere, the solution was poured into 100 mL of toluene. The product was obtained as white flakes. After being washed with hot deionized water and methanol, alternating several times, the product was treated in a Soxhlet extractor with alcohol under reflux. After drying in vacuo at 80 °C for 15 h, 9.3 g of pure SPAE-3 was obtained. Yield: 90%.

All the other polymers were synthesized using the same procedure.

SPAE series. FT-IR (KBr): 1034 cm^{-1}, 1127 cm^{-1} (–SO_3Na), 1660 cm^{-1} (C=O).

SPAE-1. ^{1}H NMR (300 MHz, DMSO-d_6) δ (ppm): 7.80 (m, 3.4H), 7.51 (d, *J* = 6.7 Hz, 2H), 7.41 (s, 1H), 7.07 - 6.77 (m, 13.4H), 6.68 (d, *J* = 8.0 Hz, 2H),4.21 (s, 2H), 4.11 (s, 2H), 2.12 (s, 2H).

SPAE-2. ^{1}H NMR: 7.80 (m, 2.88H), 7.51 (d, *J* = 6.7 Hz, 2H), 7.41 (s, 1H), 7.07 - 6.77 (m, 12.88H), 6.68 (d, *J* = 8.0 Hz, 2H), 4.21 (s, 2H), 4.11 (s, 2H), 2.12 (s, 2H).

SPAE-3. ^{1}H NMR: 7.80 (m, 2.36H), 7.51 (d, *J* = 6.7 Hz, 2H), 7.41 (s, 1H), 7.07 - 6.77 (m, 12.36H), 6.68 (d, *J* = 8.0 Hz, 2H), 4.21 (s, 2H), 4.11 (s, 2H), 2.12 (s, 2H).

SPAEN series. FT-IR (KBr): 1034 cm^{-1},1127 cm^{-1} (–SO_3Na), 1660 cm^{-1} (C=O), 2230 cm^{-1}(–CN).

SPAEN-1. ^{1}H NMR: 7.84 (d, *J* = 8.0 Hz, 2H), 7.50 (d, *J* = 8.3 Hz, 2H), 7.41 (m, 1H), 7.23-6.49 (m, 15.41H), 4.21 (s, 2H), 4.12 (s, 2H), 2.17 (s, 2H).

SPAEN-2. ^{1}H NMR: 7.84 (d, *J* = 8.0 Hz, 2H), 7.50 (d, *J* = 8.3 Hz, 2H), 7.41 (m, 1H), 7.23-6.49 (m, 14.81H), 4.21 (s, 2H),4.12 (s, 2H), 2.17 (s, 2H).

SPAEN-3. ^{1}H NMR 7.84 (d, *J* = 8.0 Hz, 2H), 7.50 (d, *J* = 8.3 Hz, 2H), 7.41 (m, 1H), 7.23-6.49 (m, 14.33H), 4.21 (s, 2H), 4.12 (s, 2H), 2.17 (s, 2H).

2.4. Membrane Preparation

Sodium-form copolymer (1.0 g) was dissolved in dimethylacetamide (DMAc, 10 mL) overnight. Next, the solution was filtered with a fine glass frit filter funnel and cast directly onto clean glass plates. After being carefully dried at 60 °C for 10 h and vacuum-dried at 120 °C for 24 h, tough and flexible films of sodium-form polymer were obtained. The membranes were transformed to the acid-form copolymer by proton exchange in 1 M H_2SO_4 for 24 h at room temperature. The membranes were soaked and washed thoroughly with deionized water. The thickness of membranes was in the range of 60-80 μm.

3. Measurements

4.

3.1. Instruments

The polymer viscosities were determined using an Ubbelohde viscometer in thermostatic container with the polymer concentration of 0.5 g dL^{-1} in N-methylpyrrolidone (NMP) at 25 ± 0.1 ^{o}C. FT-IR spectra were measured on a Nicolet Impact 410 Fourier-transform infrared spectrometer. ^{1}H NMR and ^{13}C NMR experiments were carried out on a Bruker 510 spectrometer (300 MHz for ^{1}H, 75 MHz for ^{13}C) using DMSO-d_6 as solvent.

Differential scanning calorimeter (DSC) measurements were performed on a Mettler Toledo DSC821^{e} instrument at a heating rate of 20 °C min^{-1} from 50 to 300 ^{o}C under nitrogen. Thermogravimetric analysis (TGA) was employed to assess thermal stability of membranes with a Netzch Sta 449c thermal analyzer system. Before analysis, the films were dried and kept in the TGA furnace at 120 °C in a nitrogen atmosphere for 30 min. The samples were cooled to 100 °C and then reheated to 800 °C at 10 ^{o}C min^{-1}, and the temperatures at 5% and 10% weight loss were recorded for each sample.

3.2. Water Uptake and Swelling Ratio Measurements

A piece of membrane was vacuum dried at 120 °C to a constant weight, which was recorded as W_{dry} and then immersed in deionized water at different selected temperatures. During this period, the wet membrane was quickly weighed several times after removing surface water with tissue paper until a constant weight was obtained, which was recorded as W_{wet}.

The water uptake was reported using water weight percent of dry membranes as follows:

$$\text{Water uptake (\%)} = [(W_{wet} - W_{dry})/W_{dry}] \times 100\%$$

The swelling ratio was calculated from the change of membrane length by

$$\text{Swelling ratio (\%)} = [(L_{wet} - L_{dry})/L_{dry}] \times 100\%$$

Where L_{wet} and L_{dry} are the lengths of the wet and dry membranes, respectively.

3.3. Lambda Number

The lambda value (λ) indicates the number of water molecules absorbed per sulfonic acid group and is expressed as:

$$\lambda_w = [(W_{wet} - W_{dry})/M_{H2O}]/[IEC \times W_{dry}]$$

where M_{H2O} is the molecular weight of water (18.01 g mol^{-1}) and weight-based ion-exchange capacity (IEC) is the ion exchange capacity of the dry membranes in equivalents per gram. The lambda number, like proton conductivity, scales with the ion exchange capacity [34].

3.4. Ion-exchange Capacity (IEC) of Membranes

The experimental IEC values of pure and the membranes were determined by classical titration [34, 35]. Membrane samples (about 0.06 g) were immersed in 2 M NaCl solution for at least 24 h to liberate the H^+ ions (the H^+ ions in the membranes

were replaced by Na^+ ions). The exchanged protons within the solutions were titrated with 4 mM NaOH aqueous solution by using phenolphthalein as an indicator. For each sample, at least three measurements were carried out until the titration reached to a constant value. The IEC value was calculated from the titration result via the following formula: IEC (mequiv g^{-1}) = (consumed mL NaOH × molarity NaOH)/W_{dry}

3.5. Oxidative and Hydrolytic Stability

A small piece of the membrane sample was soaked in Fenton's reagent (3% H_2O_2 containing 2 ppm $FeSO_4$) at 80 °C. The stability was evaluated by recording the retained weights of membranes after treating in Fenton's reagent for 1 h and the time when the membranes disappeared.

3.6. Proton Conductivity

The proton conductivity was measured by a four-electrode ac impedance method from 0.1 Hz to 100 kHz, 10 mV ac perturbation and 0.0 V dc rest voltage using a Princeton Applied Research Model 273A Potentiostat (Model 5210 frequency response detector, EG&GPARC, Princeton, NJ). The membranes were fixed in a measuring cell which was made of two outer gold wires to feed current to the sample and two inner gold wires to measure the voltage drops. The specimens were soaked in deionized water for at least 24 h prior to testing. Conductivity measurements of fully hydrated membranes were carried out with the cell immersed in liquid water, as reported in previous work [36]. The proton conductivity was calculated by the following formula:

$$\sigma = L/RA$$

where L was the distance between the electrodes, R was the membrane resistance and A was the cross-sectional area of membrane.

3.7. Morphology

TEM images were determined by JEM-2000EX. Before test, the polymers were converted into Pb^{2+} forms (SPAE- Pb and SPAEN- Pb) by immersing the polymers in $Pb(COOH)_2$ solutions for 24 h. The stained membrane was embedded in epoxy resin and sectioned using a microtome to yield 50 nm thick samples，which were then placed on copper grids. Images were taken on an ultrahigh-resolution transmission electron microscope (JEOLJEM-2010FEF) using an accelerating voltage of 200 kV.

4. Results and Discussion

4.1. Synthesis and Characterization of the Sulfonated Monomer

As shown in Scheme 2, a two-step route was used to synthesize a carbonyl-activated difluoro-monomer (SDPPM). SDPPM was prepared by an aluminum chloride catalyzed Friedel-Crafts acylation of 1,3-diphenoxyalkanes with 2,6-difluorobenzoyl chloride to yield DPPM, followed by a sulfonation reaction with chlorosulfonic acid at room temperature for 24 h. Under these conditions, the sulfonation reaction was expected to occur primarily at the position para- to the ether

linkage of DPPM, because electronic and steric effects made this position more reactive than other sites. ^{1}H NMR and FT-IR spectra characterization confirmed the chemical structures of DPPM and SDPPM (Figure 1 and Figure 2).

4.2. Synthesis and Characterization of Sulfonated Poly(arylene ether)s.

The preparation of comb-shaped sulfonated poly(arylene ether)s was carried out by K_2CO_3-mediated nucleophilic polycondensation reaction. As shown in Scheme 3, 2,6-difluorobenzonitrile, 4,4'-dihydroxyldiphenylether and SDPPM were polymerized in tetramethylene sulfone (TMS), and toluene was used to dehydrate the reaction system. The reaction temperature was first controlled at 140 °C to remove the water generated during the bisphenoxide formation, and then increased slowly to 180 °C by removal of toluene to accomplish polymerization. The degree of sulfonation (DS) of the polymer is defined as the ratio of the number of sulfonate groups per average repeat unit of copolymer. The polymers with different DS values could be obtained by adjusting the feed ratio of the sulfonated monomer (DFSDE) to the unsulfonated monomer (2,6-difluorobenzonitrile). SPAE polymers with relatively high DS of 0.74-0.92 were synthesized for fabrication of membranes with adequate proton conductivities. Selected properties of the polymers, such as viscosity and ion exchange capacity, are listed in Table 1. The viscosities of the sulfonated polymers were in the range of 0.73-1.08 dL g^{-1}, which indicated the polymerization had been conducted successfully despite the existence of bulky pendant groups in DFSDE. All of the sulfonated polymers were soluble in polar aprotic solvents, such as DMSO, NMP, DMAc and dimethylformamide (DMF).

The chemical structures of SPAE polymers were confirmed by FT-IR and ^{1}H NMR spectroscopies. As shown in FT-IR spectra (Figure 3), SPAE polymers showed characteristic bands at around 1034 cm^{-1} and 1127 cm^{-1}, assigned to the O=S=O stretching vibration of sulfonate groups. The absorption at 1662 cm^{-1} corresponding to stretching vibrations of diphenylcarbonyl segments was also observed in the spectra of SPAE series. These results confirmed successful introduction of the sulfonated groups onto the polymer side chains. Figure 4 shows the ^{1}H NMR stacked spectra of SPAE-1,2 and 3. As expected, the resonance signals of the ortho sulfonyl and carbonyl protons appear at higher frequencies than those of the electron-rich protons such as the ortho ether linkage protons, because of deshielding from the sulfonyl or carbonyl groups. Alkyl protons appear at the lowest frequencies. The DS values were calculated by comparing the intensity of the unique sulfonated polymer's H_1 proton with the intensity value of the proton in a non-sulfonated polymer's H_{10} protons. The following equation determines the DS from the ratio of experimental integral values compared with the ratio of expected number of protons per average repeat unit:

$$R=2I_3 + 4I_{10}=2I_1 + 4I_1(1-DS)/DS$$

Therefore, $DS=4I_1/2I_1 + R$

Here DS is the degree of sulfonation (0-1), R is the integral value from 7.69-7.89 ppm, I_1 is the intensity of H_1, I_3 is the intensity of H_3, and I_{10} is the intensity of H_{10} (in Figure 4).

The calculated results are listed in Table 1. The experimental DS values of these

sulfonated copolymers determined by ^{1}H NMR were almost the same as the calculated ones expected from the feed ratio of the sulfonated monomer, which indicated that the sulfonate content of the obtained copolymers are well controlled.

The chemical structures of SPAEN were also confirmed by FT-IR and ^{1}H NMR spectroscopes. As shown in FT-IR spectra (Figure 3), SPAEN copolymers showed a characteristic band at 1034 cm^{-1} assigned to O=S=O stretching vibration of sulfonate groups. The bands at 1662 cm^{-1} corresponding to stretching vibrations of diphenylcarbonyl segments and those at 2230 cm^{-1} corresponding to stretching vibrations of nitrile group were also observed in the spectra of SPAEN series.

The structures were further confirmed by ^{13}C NMR spectra. The carbon signal of the alkyl groups appeared at the lowest frequencies from 28 ppm to 64 ppm. The signal of the carbon in the nitrile group was observed at 114 ppm. In addition, some characteristic proton and carbon signals arising from sulfonated side chains were also clearly identified.

The structures of SPAEN copolymers were confirmed by ^{1}H NMR spectra (Figure 5), which was also used to monitor the DS (Table 1).

4.3. Thermal Properties

Thermal properties of SPAE membranes and SPAEN membranes in sodium and acid forms were evaluated by DSC and TGA. The measured results are shown in Table 2. The glass transition temperatures (T_g) values of the sodium-form both SPAE and SPAEN increased from 206 to 228 °C when the DS increased. This is because the introduction of sulfonate groups increased the intermolecular interactions by pendant ions or hydrogen bonding and molecular bulkiness, which hindered the internal rotation of the chain segments and led to increased T_g for the sulfonated polymers. No obvious T_g could be observed for the acid-form SPAE and SPAEN in our experiments.

The thermal stability of the sulfonated polymers in acid form was investigated by TGA. All the samples were pre-heated at 120 °C for 30 min in the TGA furnace to remove moisture. The $T_{d5\%}$ and $T_{d10\%}$, at which the polymer loses 5 wt.% and 10 wt.%, are summarized in Table 2, and the $T_{d5\%}$ and $T_{d10\%}$ decreases with increasing DS value. As shown in Figure 6, all the TGA plots exhibit two-stage decompositions. The first stage at around 200–290 °C was possibly associated with the loss of bound water and degradation of the sulfonic acid groups, while the second stage at around 400 °C was likely related to the degradation of main chains.

4.4. IEC, Water uptake and dimensional swelling

IEC plays a critical role in determining the proton conductivity of the membranes. The experimental IEC values determined by the acid–base titrations were in the range of 1.29-1.5 mequiv g^{-1}, which were in good agreement with the calculated IEC values (Table 1). This indicated that the sulfonated monomers were successfully incorporated to the polymer backbone by polycondensation.

The water uptake and swelling ratio of PEMs are very important properties that to a large degree determine their proton conductivities, mechanical strength, and other properties. An appropriate amount of water within membranes is required to facilitate

proton transport, but excessive water absorption increases the dimensional swelling excessively, leading to a severe loss of mechanical strength. Therefore, the preparation of sulfonated polymers with appropriate water uptake and dimensional stability is one of the critical requirements for their application as PEMs. In this study, the special side-chain-sulfonated structure of SPAE and SPAEN, which contained the flexible linkages to separate the hydrophilic sulfonic acid unit and the hydrophobic polymer main chain, was expected to provide a good approach to limit the dimensional swelling and to control the morphology.

Water uptake and swelling ratio data of membranes are listed in Table 3. As expected for both series of membranes, the water uptake and the swelling ratio increased with DS and temperature. Despite their relatively high DS, SPAE-3 and SPAEN-3 showed less than 70% water uptake and less than 26% swelling ratio at 100 °C, which ensured good dimensional stability at high temperature.

Interestingly, the SPAEN membranes displayed much lower dimensional swelling and water uptake than the SPAE membranes with an equal IEC, which could be attributed to the introduction of cyano groups in the main chain of PAEN (Figure 7 and 8). These cyano groups may increase the interactions of the polymer main chains [37,38].

4.5. *Oxidative Stability*

To evaluate whether SPAE and SPAEN membranes are capable of withstanding strong oxidizing environments during the fuel cell operation, their oxidative stability was measured as the time required for membrane samples to start disintegrating during immersion in Fenton's reagent at 80 °C, and the weight retention after treatment in Fenton's reagent at 80 °C for 1 h. The oxidative stability results are given in Table 1. All the membranes had a weight retention of >97% after treatment and maintained their dimensional form within 8 h, suggesting that the membranes had excellent oxidative stability.

4.6. Proton Conductivity and Methanol Permeability

Before proton conductivity measurements, all membranes were initially hydrated by immersion in deionized water for 24 h at room temperature. Proton conductivities of all the hydrated membranes were measured in the temperature range of 20–100 °C under 100% RH and are plotted as a function of temperature in Fig. 9. As seen, the conductivity increases with increasing temperature and IEC. SPAE-3 membrane (IEC = 1.5 mequiv g^{-1}) exhibited high conductivity of 0.023 S cm^{-1} at room temperature and 0.12 S cm^{-1} at 100 °C, which was comparable to Nafion 117. Water uptake content of PEMs also plays an important role on proton conductivity. SPAE membranes displayed higher proton conductivities in comparison with the SPAEN membranes with an equal IEC. The probable reason is that the former polymers have higher water uptake than the latter.

Low methanol permeability is critical for practical use of the membranes in DMFC [39]. The methanol permeability of the membranes was measured at room temperature, and the results are given in Table 4. As seen, the methanol permeability

increases with increasing IEC and water uptake, indicating that the methanol transport across the membranes is strongly dependent on the water uptake content. As seen in Table 4, the methanol permeability values of SPAE and SPAEN at room temperature were in the range of 1.2×10^{-8} - 3.2×10^{-7} cm^2 s^{-1}, which is several times lower than the value of Nafion 117 of 1.55×10^{-6} cm^2 s^{-1}. Pivovar et al. suggested evaluating membranes according to a plot of the logarithm of the proton conductivity as the ordinate and the logarithm of the reciprocal of methanol permeability as the abscissa [40]. Figure 10 shows the relationship of proton conductivity at 80 °C and the inverse of methanol permeability for the polymeric films; a line of slope=(1) is included depicting constant selectivity through the point of Nafion 117, according to reference [40]. All the membranes of the present study were located to the upper-right of the line, which implies their higher selectivity in comparison with Nafion 117.

4.7. Morphology of the Membranes

Proton conductivity and dimensional stability of the membranes are closely related to their morphology. Ion channels formed by hydrophilic domains are helpful to the movement of protons. In order to observe nanophase-separated morphology of SPAE membranes, the TEM analysis was performed on Pb^{2}+ stained SPAE and SPAEN ultrathin membranes on the carbon grid under ambient humidity. Four micrographs corresponding to the morphologies of SPAE-1,3 and SPAEN-1,3 are shown in Figure 11. The dark regions represent localized ionic domains and the light regions represent the domains formed by hydrophobic polymer backbones. The images exhibited ionic groups stained by lead dispersed throughout the polymers. With the increase of DS, the lead clusters became more obvious and their density increased. This result indicated that a higher degree of sulfonation resulted in more and larger ionic domains, which might be greatly helpful to proton transport.

5. Conclusions

A series of novel sulfonated poly(arylene ether)s bearing aliphatic-chain-linked sulfophenyl pendants have been prepared as proton conductive materials. The generated membranes exhibited improved thermo-oxidative stability and dimensional stability. Some of the sulfonated polymers had combinations of high proton conductivities and low methanol permeabilities. For example, SPAE-3 with IEC~1.5 mequiv g^{-1} showed a proton conductivity of 0.12 S cm^{-1} at 100 °C, and its swelling ratio in water at 100 °C was only about 26%. It was interesting to observe obvious hydrophobic/hydrophilic phase separation morphology, which may be highly related with their good proton transport ability. The property data for some of the polymers illustrated that both SPAE-3 and SPAEN-3 might be potentially useful as polymer electrolyte membranes.

Acknowledgements

Financial support for this project was provided by the National Natural Science Foundation of China (No.: 50973040) and the Science and Technology Development Plan of Jilin Province, China (No.: 20100706 and 20090322), the Scientific Research

Foundation for the Returned Overseas Chinese Scholars, State Education Ministry (No.: 5043C1116801412), Industrial Technology Research and Development Funds of Jilin Province (No.: 2011004-1) and the Fundamental Research Funds for the Central Universities of Jilin University (No.: 421031561412). Partial support under grant R31-2008-000-10092-0 by the WCU (World Class University) program, National Research Foundation (Korea) is acknowledged.

References

[1] M.A. Hickner, H. Ghassemi, Y.S. Kim, B.R. Einsla, J.E. McGrath, Chem. Rev. 104 (2004) 4587-4612.
[2] K. Miyatake, Y. Chikashige, E. Higuchi, M. Watanabe, J. Am. Chem. Soc. 129 (2007) 3879–3887.
[3] T.J. Peckham, J. Schmeisser, S. Holdcroft, J. Phys. Chem. B 112 (2008) 2848-2858
[4] B.C.H. Steele, A. Heinzel, Nature (London) 414 (2001) 345–352.
[5] B.J. Liu, D.-S. Kim, M.D. Guiver, Y.S. Kim, B.S. Pivovar, in "Membranes for Energy Conversion", volume 2 of "Membrane Technology" series, K.-V. Peinemann, S. P. Nunes, Eds.,Wiley – VCH, chapter 1, pp. 1 – 45, February 2008.
[6] J. Jouanneau, R. Mercier, L. Gonon, G. Gebel, Macromolecules 40 (2007) 983–990.
[7] M. Rikukawa, K. Sanui, Prog. Polym. Sci. 25 (2000) 14631502.
[8] M.A. Hickner, Cy.H. Fujimoto, C.J. Cornelius, Polymer 47 (2006) 4238–4244.
[9] B.J. Liu, G.P. Robertson, M.D. Guiver, Z.Q. Shi, T. Navessin, S. Holdcroft, Macromol. Rapid Commun. 27 (2006) 1411-1417.
[10] B.J. Liu, G.P. Robertson, D.S. Kim, M.D. Guiver, W. Hu, Z. Jiang, Macromolecules 40 (2007) 1934–1944.
[11] B.J. Liu, M. Guiver, in Solid-state proton conductors: properties and applications in fuel cells, M. L. Di Vona, P. Knauth, Eds., John Wiley and Sons Ltd., Chichester, UK, 2011, Chapter 9, pp 331 – 369.
[12] J.A. Kerres, J. Membr. Sci. 185 (2001) 3–27.
[13] D.S. Kim, G.P. Robertson, M.D. Guiver, Macromolecules 41 (2008) 2126–2134.
[14] R. Nolte, K. Ledjeff, M. Bauer, R. Mulhaupt, J. Membr. Sci. 83 (1993) 211–220.
[15] K. Miyatake, H. Zhou, M.Watanabe, Macromolecules 37 (2004) 4956–4960.
[16] E.M.W. Tsang, Z.B. Zhang, Z.Q. Shi, T. Soboleva, S. Holdcroft, J. Am. Chem. Soc. 129 (2007) 15106–15107.
[17] D.J. Jones, J. Rozière, J. Membr. Sci. 185 (2001) 41–58.
[18] B. Liu, W. Hu, C. Chen, Z. Jiang, W. Zhang, Z. Wu, T. Matsumoto, Polymer 45 (2004) 3241–3247.
[19] N. Asano, M. Aoki, S. Suzuki, K.Miyatake, H. Uchida, M.Watanabe, J. Am. Chem. Soc. 128 (2006) 1762–1769.
[20] J. Jouanneau, R. Mercier, L. Gonon, G. Gebel, Macromolecules 40 (2007) 983–990.
[21] Y. Yin, J. Fang, H. Kita, K. Okamoto, Chem. Lett. 32 (2003) 328–329.

[22] K.D. Kreuer, S.J. Paddison, E. Spohr, M. Schuster, Chem. Rev. 104 (2004) 4637–4678.
[23] Z. Hu, Y. Yin, S. Chen, O. Yamada, K. Tanaka, H. Kita, K. Okamoto, J. Polym. Sci.,A: Polym. Chem. 44 (2006) 2862–2872.
[24] T. Kobayashi, M. Rikukawa, K. Sanui, N. Ogata, Solid-State Ionics 106 (1998) 219–225.
[25] C.H. Fujimoto, M.A. Hickner, C.J. Cornelius, D.A. Loy, Macromolecules 38 (2005) 5010–5016.
[26] Y.S. Yang, Z.Q. Shi, S. Holdcroft, Macromolecules 37 (2004) 1678.
[27] A. Roy, H.S. Lee, J.E. McGrath, Polymer 49 (2008) 5037–5044.
[28] Y. Chen, R.L. Guo, C.H. Lee, M. Lee, J.E. McGrath, Int. J. Hydrogen Energy, 37 (2012) 6132-6139.
[29] Y. Yang, S. Holdcroft, Fuel Cells 5 (2005) 171–186.
[30] N. Li, S.Y. Lee, Y.-L. Liu, Y.M. Lee, M.D. Guiver, Energy Environ. Sci., 5 (2012) 5346-5355.
[31] T.B. Norsten, M.D. Guiver, J. Murphy, T. Astill, T. Navessin, S. Holdcroft, B.L. Frankamp, V.M. Rotello, J. Ding, Adv. Funct. Mater. 16 (2006) 1814–1822.
[32] N. Li, C. Wang, S.Y. Lee, C.H. Park, Y.M. Lee, M.D. Guiver, Angew. Chem. Int. Ed., 123 (2011) 9158 – 9161
[33] K. Yamamoto, M. Jikei, K. Miyatake, J. Katoh, H. Nishide, E.Tsuchida, Macromolecules 27 (1994), 4312-4311.
[34] M. M. Guo, B. Liu, S.W. Guan, L. Li, C. Liu, Y.H. Zhang, Z.H. Zhang, J. Power Sources 195 (2010) 4613–4621.
[35] R. Perrin, M. Elomaa, P. Jannasch, Macromolecules 42 (2009) 5146–5154.
[36] T. Kobayashi, M. Rikukawa, K. Sanui, N. Ogata, Solid-State Ionics 106 (1998) 219–225.
[37] D.S. Kim, Kim YS, M.D. Guiver, B.S. Pivovar, J. Membrane. Sci. 321 (2008). 199–208.
[38] Y. Gao, G. P. Robertson, M. D. Guiver, S. D. Mikhailenko, X. Li, S.Kaliaguine Polymer, 47 (2006) 808–816.
[39] H.L. Cai, K. Shao, S.L. Zhong, C.J. Zhao, G. Zhang, X.F. Li, H. Na, J. Membr. Sci. 297(2007) 162.
[40] B.S. Pivovar, Y.X. Wang, E.L. Cussler, J. Membr. Sci. 154 (1999) 155–162.

Figure Captions

Table 1. Properties of copolymers.
Table 2. Thermal properties of copolymer.
Table 3. Water uptake and swelling ratio of copolymer membranes.

Scheme 1. Schematic illustrations of the different types of sulfonated polyarylethers: A) main-chain-acid SPAE; B) sulfophenylated PAE; C) SPAE having flexible side-chains.
Scheme 2. Synthesis of a carboxyl-activated difluoro-monomer bearing a sulfonate group.
Scheme 3. Synthesis route of comb-shaped sulfonated poly(arylene ether)s.

Fig. 1. ^{1}H NMR spectra of SDPPM and DPPM.
Fig. 2. FT-IR spectra of SDPPM and DPPM.
Fig. 3. FT-IR spectra of SPAE-1 and SPAEN-1.
Fig. 4. ^{1}H NMR spectra of SPAE series.
Fig. 5. ^{1}H NMR spectra of SPAEN series.
Fig. 6. TGA curves of membranes.
Fig. 7. Water swelling ratio of SPAE and SPAEN membranes as a function of temperature.
Fig. 8. Water uptake of SPAE and SPAEN membranes as a function of temperature.
Fig. 9. Proton conductivity of SPAE and SPAEN membranes as a function of temperature.
Fig. 10. Proton conductivity versus methanol resistance of membranes.
Fig. 11. Morphology of SPAE-1,3 and SPAEN -1,3 ionomers studied by TEM.

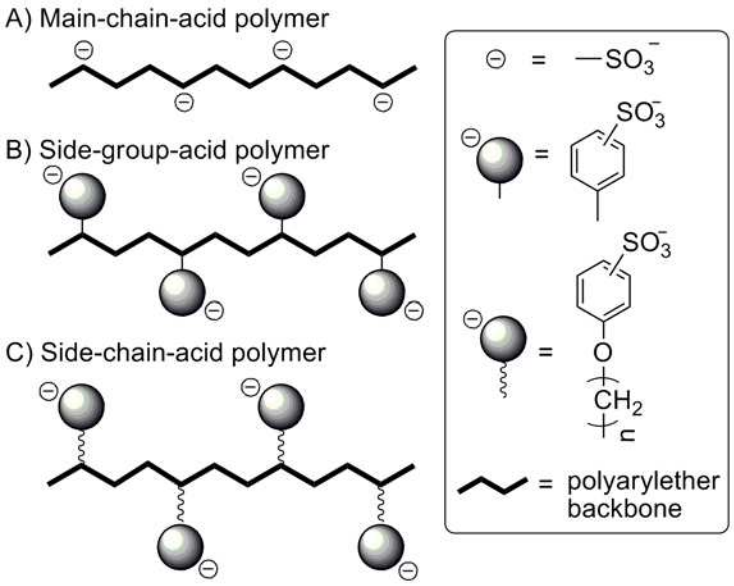

Scheme 1. Schematic illustrations of the different types of sulfonated polyarylethers: A) main-chain-acid SPAE; B) sulfophenylated PAE; C) SPAE having flexible side-chains.

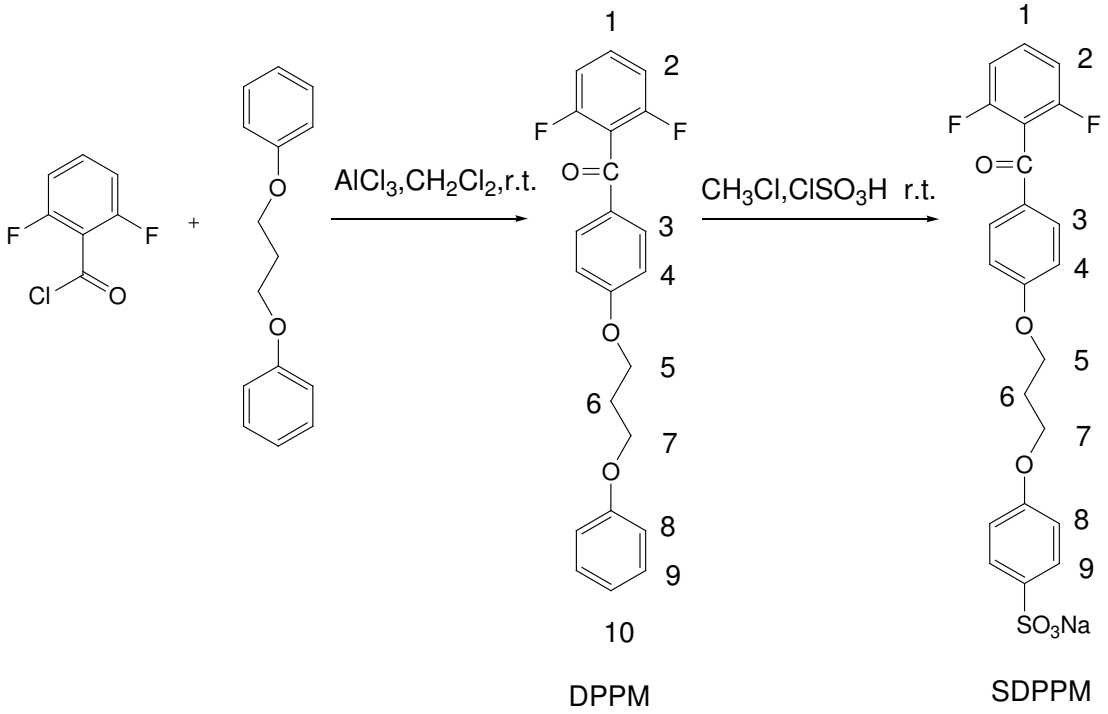

Scheme 2. Synthesis of a carboxyl-activated difluoro-monomer bearing a sulfonate group.

Scheme 3. Synthesis route of comb-shaped sulfonated poly(arylene ether)s.

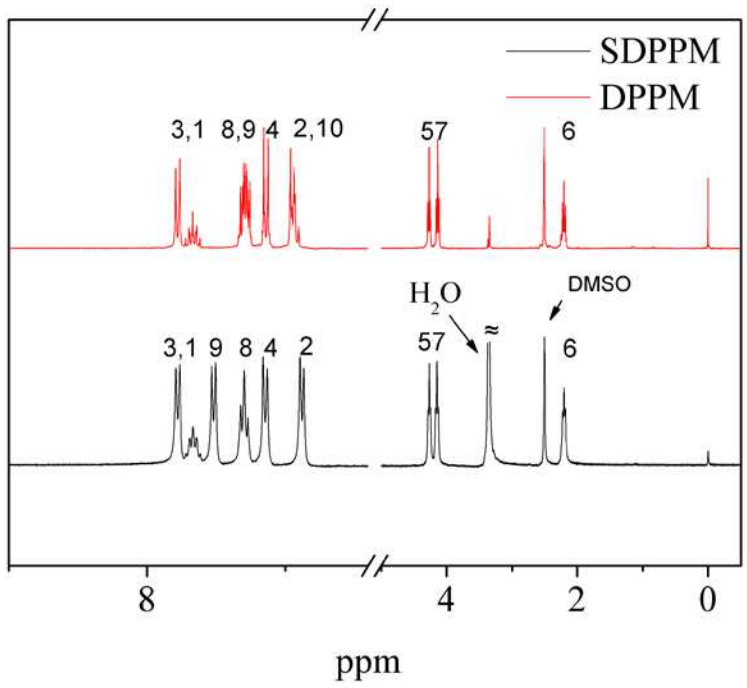

Fig. 1. ^{1}H NMR spectra of SDPPM and DPPM.

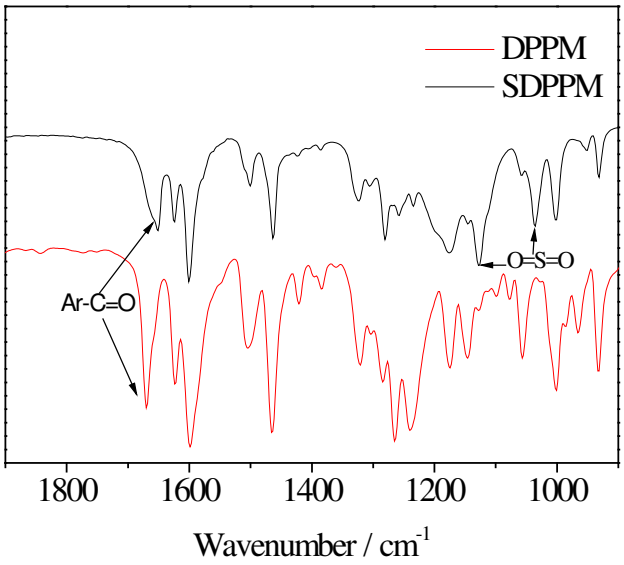

Fig. 2. FT-IR spectra of SDPPM and DPPM.

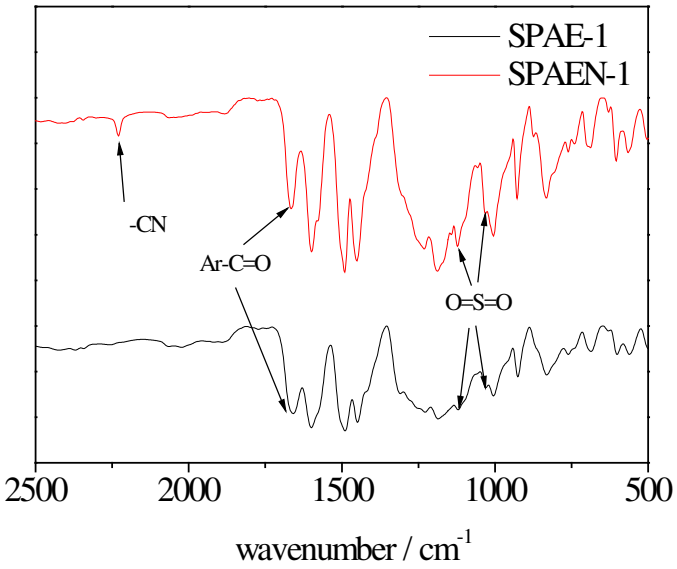

Fig. 3. FT-IR spectra of SPAE-1 and SPAEN-1.

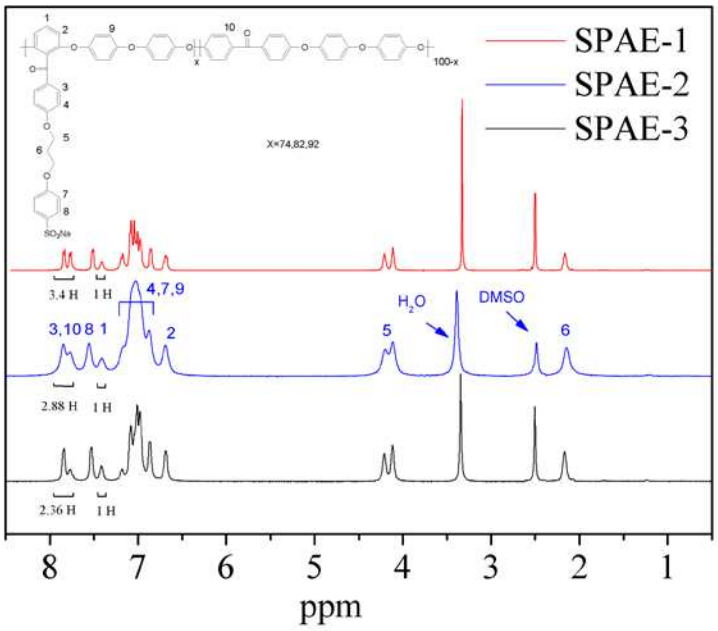

Fig. 4. ^{1}H NMR spectra of SPAE series.

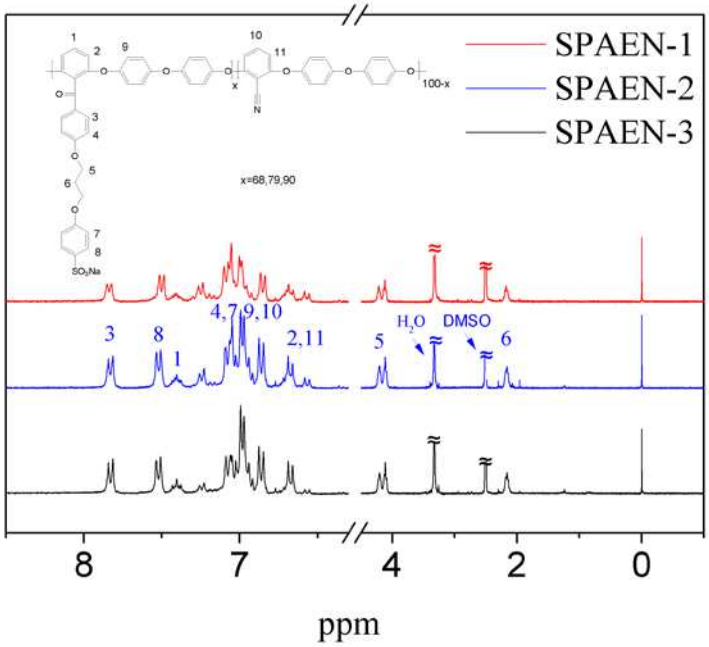

Fig. 5. ^{1}H NMR spectra of SPAEN series.

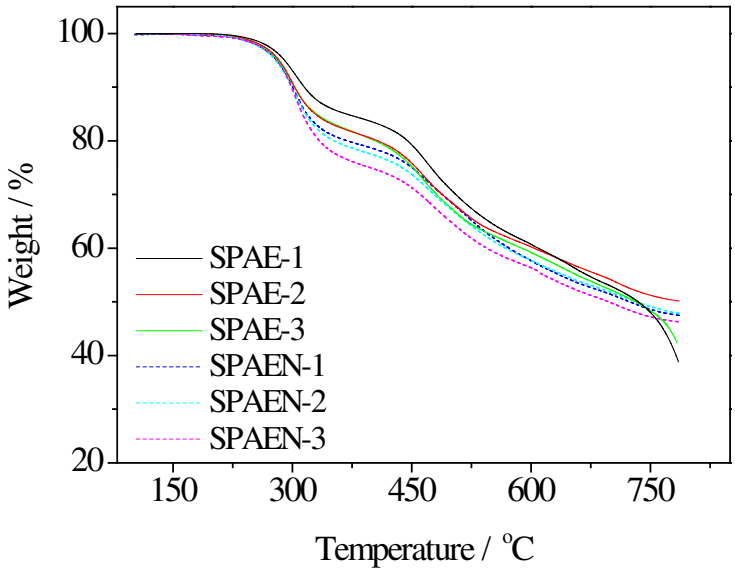

Fig. 6. TGA curves of membranes.

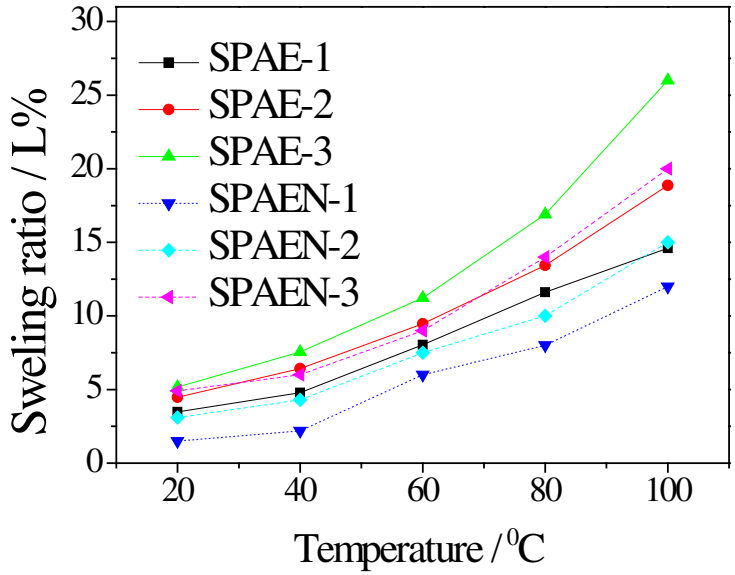

Fig. 7. Water swelling ratio of SPAE and SPAEN membranes as a function of temperature.

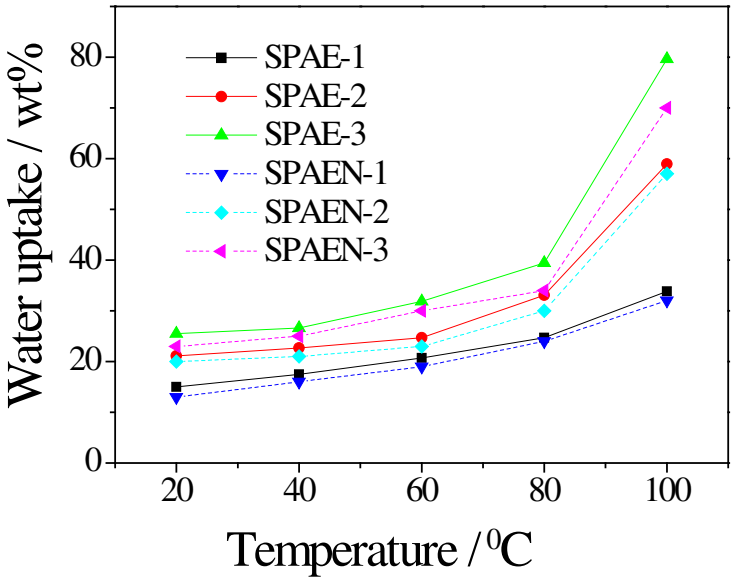

Fig. 8. Water uptake of SPAE and SPAEN membranes as a function of temperature.

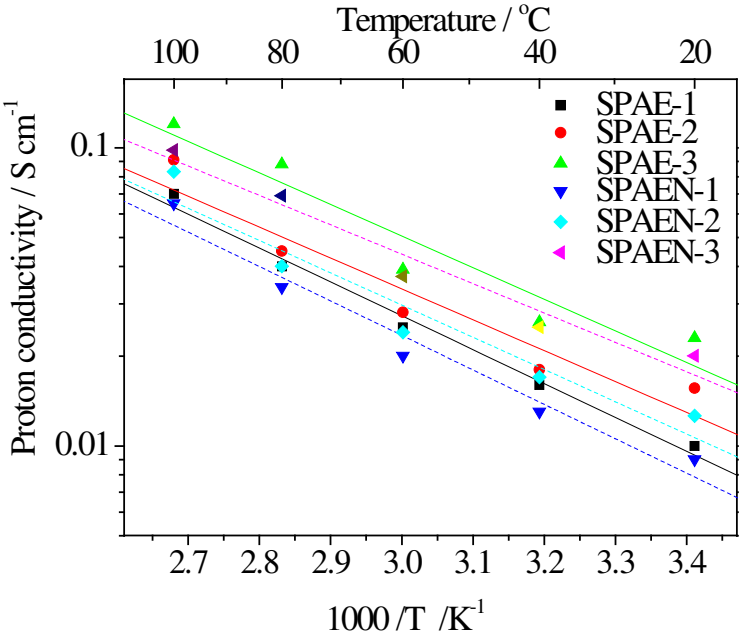

Fig. 9. Proton conductivity of SPAE and SPAEN membranes as a function of temperature.

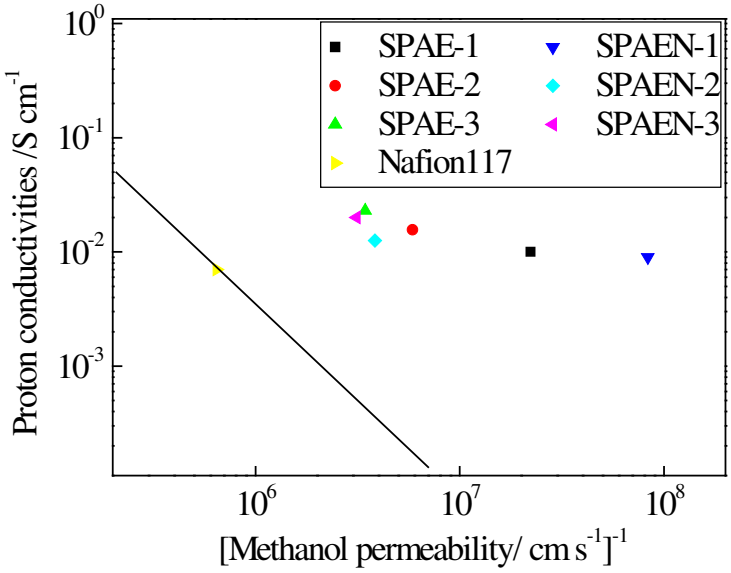

Fig. 10. Proton conductivity versus methanol resistance of membranes.

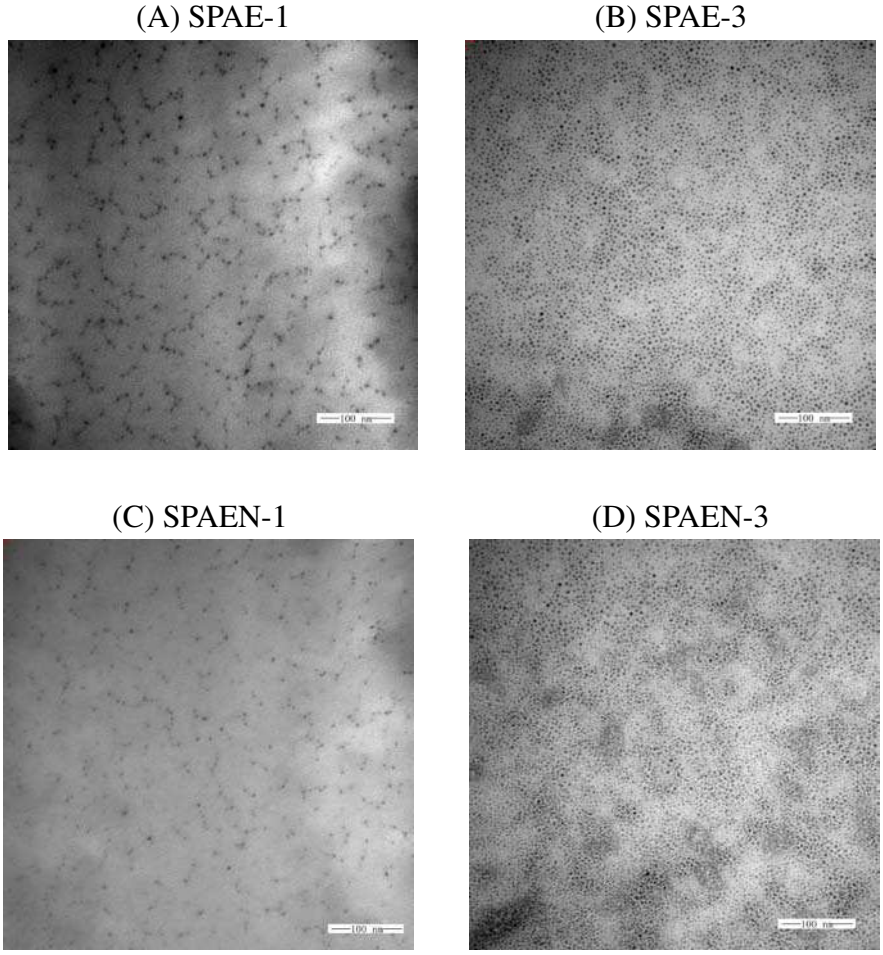

Fig. 11. Morphology of SPAE-1,3 and SPAEN-1,3 ionomers studied by TEM.

Table 1

Properties of copolymers

polymer	IEC[a]	IEC[b]	$\lambda_{w(R.T.)}$	DS[c]	η [d]	Oxidative stability	
						RW (%)[e]	RW (%)[f]
SPAE-1	1.30	1.30	6.41	0.74	1.05	99.2	>8
SPAE-2	1.40	1.39	8.37	0.82.	1.08	98.9	>8
SPAE-3	1.50	1.50	9.44	0.92	0.95	98.1	>8
PAEN-1	1.30	1.30	5.55	0.68	0.95	98.5	>8
PAEN-2	1.40	1.39	7.93	0.79	0.89	98.3	>8
PAEN-3	1.50	1.51	8.51	0.90	0.73	97.6	>8

[a] Theoretical value (mequiv g^{-1}); [b] Experimental value (mequiv g^{-1}); [c] determined by ^{1}H NMR

[d] The viscosities (dL g^{-1}) were determined using an Ubbelohde viscometer in thermostatic container with the polymer concentration of 0.5 g dL^{-1} in NMP at 25 ± 0.1 °C.

[e] Retained weights of membranes after treating in Fenton's reagent for 1 h;

[f] The disintegration time of polymer membranes in h.

Table 2

Thermal properties of copolymer

polymer	$T_{g\,(acid)}$ (°C) [a]	$T_{d\,(5\%)}$ (°C)	$T_{d\,(10\%)}$ (°C)
SPAE-1	213	290	315
SPAE-2	224	283	303
SPAE-3	226	281	301
SPAEN-1	206	280	300
SPAEN-2	215	279	299
SPAEN-3	228	278	298

[a] at a heating rate of 20 °C min^{-1} from 50 °C to 300 °C under nitrogen.

Table 3

Water uptake and swelling ratio of copolymer membranes

Polymer	Temperature (℃)									
	20		40		60		80		100	
	SR	WU	SR	WU	SR	WU	SR	WU	SR	WU
SPAE-1	3.4	15	4.7	17.5	8.0	20.7	11.6	24.7	14.6	33.8
SPAE-2	4.4	21.1	6.4	22.7	9.4	24.7	13.4	33.0	18.8	58.9
SPAE-3	5.1	25.4	7.5	26.6	11.2	31.8	16.9	39.4	26.0	79.6
SPAEN-1	1.5	13	2.2	16	6.1	18.9	8.0	24.0	12.0	32
SPAEN-2	3.1	20.1	4.3	21.1	7.5	23.2	10	30.0	15.1	57
SPAEN-3	4.9	23.1	6.0	24.9	9.0	30	14.1	34.4	20.0	70

SR：Swelling ratio (%)　WU：Water uptake (%)

Table 4
Proton conductivity, Ea and Methanol permeability of SPAE and SPAEN membranes

Polymer	Proton conductivity(S cm^{-1})					Ea	Methanol
	20 °C	40 °C	60 °C	80 °C	100 °C	(kJ mol^{-1})	permeability (cm^2 s^{-1})
SPAE-1	0.010	0.016	0.025	0.040	0.070	21.8	4.5×10^{-8}
SPAE-2	0.016	0.018	0.028	0.045	0.091	19.9	1.7×10^{-7}
SPAE-3	0.023	0.026	0.039	0.088	0.120	20.3	2.9×10^{-7}
SPAEN-1	0.009	0.013	0.020	0.034	0.065	22.1	1.2×10^{-8}
SPAEN-2	0.013	0.017	0.024	0.040	0.083	20.7	2.6×10^{-7}
SPAEN-3	0.020	0.025	0.037	0.069	0.098	18.9	3.2×10^{-7}